ELSEVIER

Thermochimica Acta 276 (1996) 57–77

thermochimica acta

Comparative study of the pyrolysis of almond shells and their fractions, holocellulose and lignin. Product yields and kinetics

J.A. Caballero *, R. Font, A. Marcilla

Departamento de Ingeniería Química, Universidad de Alicante, Ap. Correos 99, Alicante, Spain

Received 13 June 1995; accepted 21 November 1995

Abstract

A comparison between the thermal decomposition of almond shells and their components (holocellulose and lignin) was carried out, considering the yields of the most important products, under flash conditions, and the decomposition kinetics.

The yields of the main gaseous products obtained in the fast pyrolysis of almond shells can be reproduced from the yields obtained with holocellulose and lignin. The best results were obtained with CO, water and CO_2. The differences were greater with the minor hydrocarbons, CH_4, C_2H_6, C_2H_4, etc.

The kinetics of the slow thermal decomposition (TG–DTG) of almond shells cannot be reproduced by the sum of lignin and holocellulose. The cellulose from almond shells decomposes at lower temperatures than almond shells, and the behavior of isolated lignin is very different from that found when it forms part of the raw material, proving the importance of the interactions between its components.

Keywords: Almond shells; Holocellulose; Lignin; Pyrolysis; Thermogravimetry

1. List of symbols

B	weight of biomass at any moment in kg
B_1	weight of biomass of fraction 1 in kg of biomass of reaction 1 divided by the weight of the initial biomass
B_2	weight of biomass of fraction 2 in kg of biomass of reaction 1 divided by the weight of the initial biomass

* Corresponding author.

SSDI 0040-6031(95)02794-7

E	activation energy in kJ mol^{-1}
E_1	activation energy in reaction 1 in kJ mol^{-1}
E_2	activation energy in reaction 2 in kJ mol^{-1}
k	kinetic constant in min^{-1}
k'	kinetic constant in min^{-1}
k_{01}	pre-exponential factor in reaction 1 in min^{-1}
k_{02}	pre-exponential factor in reaction 2 in min^{-1}
n_1	reaction order in reaction 1
n_2	reaction order in reaction 2
O.F.	objective function
R	weight of residue at any time in kg
r	yield coefficient defined as kg of solid formed divided by kg of biomass decomposed
r'	yield coefficient defined as kg of solid formed divided by kg of biomass decomposed
T	temperature in K
t	time in s
V	weight of volatiles formed in kg
V.C.	variation coefficient in %
w	normalized weight at any moment (weight/initial weight)
$w_{\infty i}$	normalized weight at time infinity
w_{0i}	initial normalized weight of the fraction i
v	yield coefficient defined as kg of volatiles formed divided by kg of biomass decomposed

1. Introduction

The pyrolysis of biomass has received increasing attention because the conditions of the process can be optimized to produce pyrolytic liquid fuels, fuel gas, chemicals and active carbon [1].

The study of the different fractions of lignocellulosic materials (hemicellulose, cellulose and lignin) may give information as to the behavior of the raw material in accordance with the different proportions of its components. Shafizadeh and McGinnis [2] used TGA to determine the thermal degradation of cottonwood and its components, and concluded that the thermal behavior of the major components of a biomass could be approximately extrapolated to the original material. Similar results were obtained by Williams and Besler [3] using the TG technique with wood and its components. Maschio et al. [4] studied the thermal degradation of poplar wood and olive husks in an isothermal semi-batch moving-bed reactor, and concluded that the biomass can be analyzed as a sum of its main components. These researchers proposed that the pyrolysis behavior of a biomass can be predicted according to the following rule

$$[\text{Biomass}] = a[\text{Cellulose}] + b[\text{Lignin}] + c[\text{Hemicellulose}]$$

The terms in parentheses represent the fraction of the material or component, and a, b, c are the weight fractions of the corresponding biomass components in the virgin material.

The conclusions of Shafizadeh and McGinnis, and Maschio et al. could probably be applied to many different kinds of biomass if it were possible to isolate the cellulose and lignin from the raw materials without breaking their structure. Nevertheless, it is very difficult to separate the fractions of lignocellulosics without producing depolymerizations and structural changes. Besides, in raw material there are always interactions between the different fractions which contribute to their properties and that are obviously not present in the isolated fractions.

Thus, the objective of this paper is to compare the behavior of almond shells and their fractions, holocellulose and lignin, in the pyrolysis process, considering the composition of the products obtained and the kinetics of the thermal decomposition. To analyze the different compositions that can be obtained when lignin and holocellulose are separated or together in the almond shells, a Pyroprobe 1000 was applied under fast pyrolysis conditions, because relatively high primary yields of carbon oxides and hydrocarbons could be measured with a good accuracy. The TG technique was selected for studying the kinetics of breakdown of lignin, holocellulose and almond shells, because in slow heating rate conditions it was possible to observe separated decomposition processes in different ranges of temperatures, and so analyze and compare the kinetic behavior of the components considered.

2. Experimental

The raw material used was almond shells. Almond shells, variety marcona, were washed with water, dried, crushed and sieved to obtain a uniform material of 0.297–0.500 mm particle size. The lignin and the holocellulose were obtained from almond shells by standard methods [5–7]. The holocellulose used was Kruchner holocellulose and the lignin was Klason lignin.

The separation of lignin from a biomass is a difficult problem and all methods used cause alterations to the original structure. According to Evans et al. [8] and García et al. [9], it is impossible to isolate lignin from wood without changing its structure; even when using the same method, it is difficult to obtain identical samples. Only the method based on the enzymatic removal of carbohydrates in samples of finely milled wood seems to produce a lignin with an unmodified structure. In practice, however, this method is slow and difficult. Details on obtaining lignin can be found elsewhere (Caballero et al. [10]). The composition obtained from almond shells is the following:

cellulose, 37 wt%; hemicellulose, 32 wt%; lignin, 27 wt%; other, 4 wt%

Experiments under flash pyrolysis conditions were carried out in a Pyroprobe 1000 CDS instrument. The Pyroprobe 1000 is a pyrolyzer heated by a platinum filament which is connected in series with a gas chromatograph. A 4 m long, Porapaq Q column was used. The chromatograph apparatus has two detectors: a flame ionization detector (FID) and a thermal conductivity detector (TCD). The carrier gas was helium and the

flow rate was 45 ml min^{-1} for TCD and 26 ml min^{-1} for FID. More details on the apparatus and the chromatographic method are reported by García et al. [11]. The products analyzed were: CO, CO_2, water, methane, ethylene + acetylene, propylene, propane, methanol and acetic acid.

Data on the pyrolysis of almond shells are obtained from Devesa [12] and Font et al. [13] and were used in this work to compare them with the results obtained with the cellulose and lignin.

The kinetic analysis was carried out in a Perkin-Elmer thermobalance, model TGA7 controlled by a PC AT compatible system. The atmosphere used was nitrogen with a flow rate of 60 ml min^{-1}. A platinum sample pan, with two compartments, open to the nitrogen atmosphere, was used in the TG experiments. This sample pan allowed experiments to be carried out in which holocellulose and lignin decompose simultaneously under the same conditions, without contact between them. A first series of runs was performed at 5, 10, and 25°C min^{-1} with lignin, holocellulose and almond shells. A second series of experiments at 25°C min^{-1} was performed with different proportions of lignin and holocellulose in order to discuss the behavior of the almond shells. The weight of the sample used in all the TG experiments was around 5 mg. In all cases, the experiments were duplicated and differences in the weight measured were never higher than 2%.

3. Results

3.1. Comparison between the almond shell yields and holocellulose + lignin yields obtained with the Pyroprobe 1000

A set of experiments between 700 and 900°C was carried out with lignin and holocellulose using an analytical Pyroprobe 1000 apparatus. The pyrolysis time was 20 s and the nominal heating rate was 20°C ms^{-1}. Funazukuri et al. [14], García et al. [11], and Caballero et al. [10] deduced that the actual heating rate is within the range 300–3000°C s^{-1}. The reactant was introduced into the platinum coil of the Pyroprobe, and then heated rapidly to the final temperature and held there until the change was completed. Products from pyrolysis are analyzed by gas chromatography and the char is measured gravimetrically. Under these conditions, the residence time of the volatiles in the hot zone is only milliseconds, so the secondary reactions can be neglected. In addition, it was confirmed that the pyrolysis time was sufficient to decompose the particles completely.

The experimental yields of almond shells, lignin and holocellulose are presented in Fig. 1.

Taking into account the composition of almond shells (27% lignin and 73% holocellulose), and according to the hypothesis of Shafizadeh and McGinnis and Maschio et al., the behavior of almond shells should be the sum of lignin and holocellulose multiplied by their weight fractions in the raw material. These yields were also calculated and plotted in Fig. 1. From the comparison between the calculated yields of almond shells from their fractions and the experimental data, the following observations can be made.

(i) For water, CO_2 and CO, the almond shell yields are close to those calculated from the yields from lignin and holocellulose mixture (Figs. 1a,b,c).

(ii) The calculated yields of methane are around the mean value of the values obtained from the raw material (Fig. 1d).

(iii) From almond shells, yields of other hydrocarbons, acetic acid, and methanol + formaldehyde are higher than those calculated by adding up the yields from holocellulose and lignin (Figs. 1e,f,g).

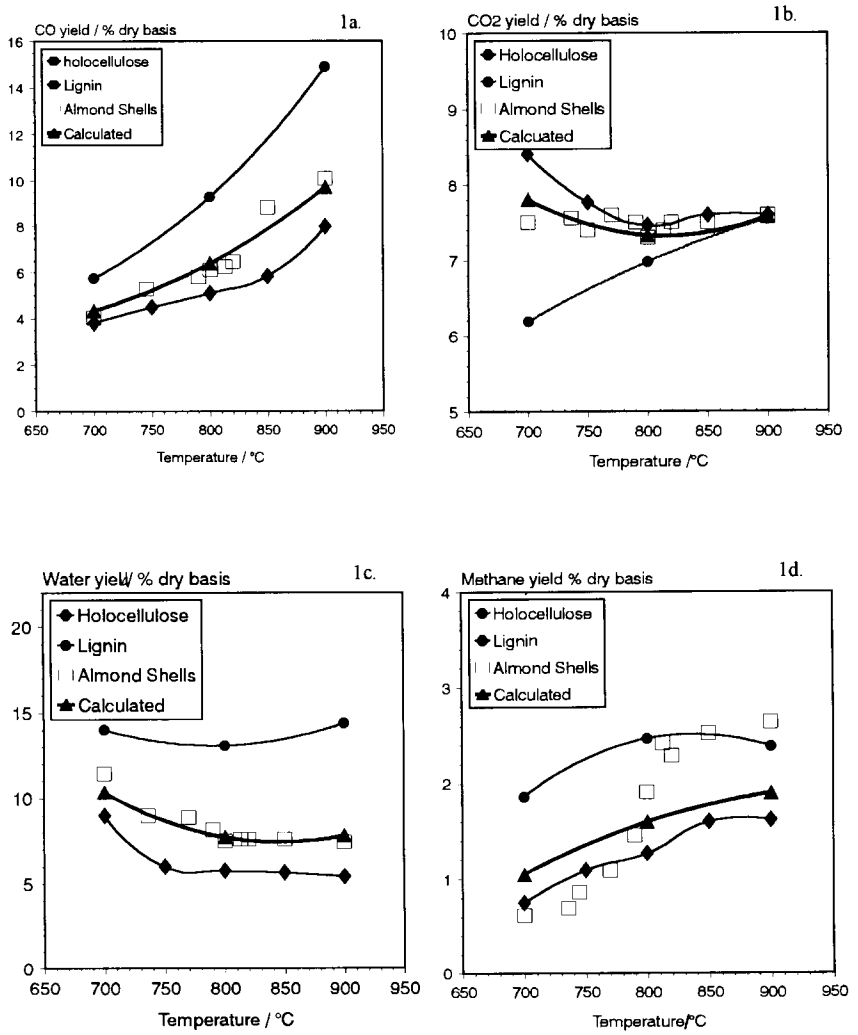

Fig. 1. Comparison between the yields of almond shells and their fractions obtained with the Pyroprobe 1000 as a function of the temperature.

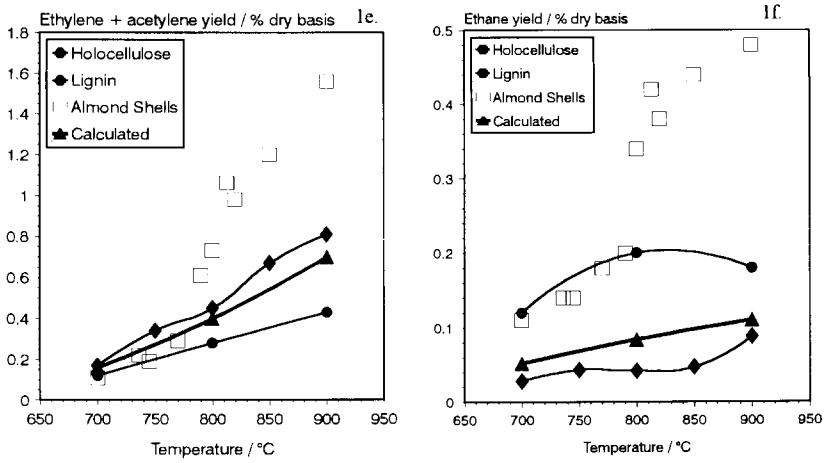

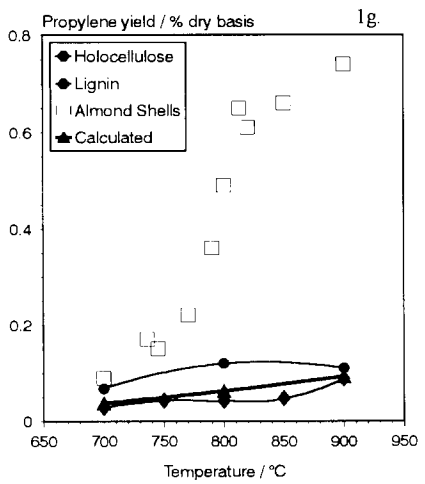

Fig. 1. (*Continued*).

It can be concluded that the final yields of CO, water and CO_2 are not significantly affected by the interactions between holocellulose and lignin in the raw material. The separation process, although altering the structure of the native lignin and holocellulose, does not modify the final yield of these compounds under flash pyrolysis conditions. In the case of CO, CO_2 and water, there is a very good agreement between the raw material values and their fractions.

The situation is somewhat different in the case of hydrocarbon yields. The hydrocarbons from almond shells undergo a great increase in yield around 800°C. This increase in yield does not coincide with the calculated values by summing the yields of lignin and holocellulose products. When pyrolyzing holocellulose and lignin, there are large

increases in the yields between 650 and 750°C [11, 12]. It is possible that in the raw material, with a greater extent of polymerization and without any pre-treatment, the temperature of decomposition is higher than when pyrolyzing its separated fractions. From these results, it seems apparent that there may be an important interaction between cellulose and lignin compounds in the hydrocarbon formation.

Compounds such as methanol and formaldehyde derive from the metoxil groups of lignin with a lesser proportion deriving from holocellulose. In previous works, García et al. [11] and Caballero et al. [10] found that these products reached their maximum yield, under flash conditions, at temperatures around 500°C and short pyrolysis times (about one second). However, these metoxil groups can be partially hydrolyzed in the separation process and this may be the reason why the methanol yield from almond shells reaches 0.78% and only 0.53% in the calculated values, and why that of acetic acid in almond shells reaches 8.7% and only 0.5% in the calculated values.

In conclusion, it can be deduced that only the yields of some compounds, such as CO, CO_2 and water, in almond shell pyrolysis are close to those deduced by adding up their fractions. However, most hydrocarbons and oxygenated compounds give altered pyrolysis yields as a consequence of the isolation process.

3.2. *Kinetic study*

Various different kinetic studies of the thermal decomposition of lignocellulosic materials have been carried out during recent decades. The kinetics of the pyrolysis process of these materials is very complex. There is a great heterogeneity in lignocellulosic materials: the composition can change considerably from one wood composition to another, e.g. in gymnosperm wood (soft woods), the amount of lignin varies between 27% and 37%, while in angiosperm wood (hard woods), the amount ranges from 16% to 29% [15]. In addition, the composition of lignin and hemicelluloses depends on the species, and in the case of lignin, its structure even varies depending on the age and part of the plant concerned.

The mechanisms of reactions can vary depending on the conditions under which pyrolysis is carried out (it is well known, for example, that under flash conditions the yield of volatiles increases and the char formed decreases), and other factors such as pressure, atmosphere of reaction, catalytic effects by impurities, etc.

Cellulose is the best known of the polymers that comprise biomass. Its structure is very well defined and the mechanisms of its decomposition have received considerable attention by researchers. Different models and kinetic constants concerning the decomposition of cellulose are proposed in the literature [16–31] under different operating conditions and using different experimental apparatus. Lignin does not have a unique structure. The dispersion of kinetic parameters is greater than for cellulose, and different kinetic models also appear [10, 32–36]. Hemicellulose is formed by different compounds, pentosanes and similar compounds. The kinetics studies concern some specific compounds that have, therefore, different kinetic constants [3, 37–39]. Table 1 shows some of the kinetic parameters for lignin, cellulose, hemicellulose and other specific compounds, the structures of which are similar to one of the fractions.

Table 1
Some kinetic constants from the literature

Author	k_0/min^{-1}	E/kJ mol^{-1}	Range of temperatures/°C	Material used
Chaterjee and Conrad [18]	3.3×10^{20}	175.7	270–310	Cotton
Lewellen et al. [30]	4.07×10^{11}	139	–	Filter paper 0.01 cm thick
Antal et al. [31]				Filter paper
2.16°C min^{-1}	2.8×10^{7}	221.1	110–600	
5.65°C min^{-1}	8.4×10^{11}	157.6	110–600	
10.9°C min^{-1}	1.6×10^{12}	148.8	110–600	
22.4°C min^{-1}	2.7×10^{12}	162.6	110–600	
55.0°C min^{-1}	4.2×10^{11}	153.0	110–600	
Varhegyi and Antal [29]	2.2×10^{9}	234 $n = 1.2$	200–450	Avicel cellulose
Arsenau [28]	–	189.7	285–320	Filter paper
		151.3	258–280	
Roberts [40]	1.8×10^{17}	200.8 $n = 1/2$	–	Cellulose
	7.3×10^{13}	175.7		
Lipska and Parker [19]	–	209.2	250–300	White α-cellulose
Conesa et al. [41]	3.01×10^{17}	217.2		Whatman no. 6 filter paper
Hajaligol et al. [42]	1.2×10^{10}	132.8	300–1000	Filter paper 0.01 cm thick
Avni and Coughlin [43]	2.66×10^{8}	if $0 < X < 0.4$[a]	100–700	Lignin
		$58.43 + 290.59X$		
		if $0.4 < X < 0.6$		
		171.62		
Stamm [44]	8.4×10^{11}	96.3	110–220	Lignin
Krieger and Chen [45]	4.7×10^{2}	25.1	160–680	Lignin
	9	30.6	410–1890	
Ramiah [39]	–	54.4	245–330	Lignin
Hirata and Hiroshi [46]	4.3×10^{12}	145.6	–	Xylan
	–	125.6		
Font et al. [47]				Almond Shells
5°C min^{-1}	8.5×10^{5}	112.0	100–700	
	8.5×10^{15}	242.1	100–700	
10°C min^{-1}	4.7×10^{5}	107.8	100–700	
	1.28×10^{16}	243.3	100–700	
25°C min^{-1}	4.8×10^{5}	106.2	100–700	
	4.98×10^{14}	225.3	100–700	
20°C min^{-1}	7.9×10^{5}	108.3	100–700	
	1.02×10^{15}	229.1	100–700	
30°C min^{-1}	4.98×10^{6}	104.5	100–700	
	8.06×10^{13}	215.3	100–700	
40°C min^{-1}	2.63×10^{5}	100.3	100–700	
	8.92×10^{12}	203.6	100–700	
10°C min^{-1}	2.43×10^{18}	256.8	100–700	Cellulose
10°C min^{-1}	2.5×10^{5}	98.3	100–700	Holocellulose
	1.56×10^{16}	230.6	100–700	
10°C min^{-1}	1.21×10^{6}	109.9	100–700	Lignin

[a] X is the conversion degree.

In the present work, the holocellulose and lignin studied were derived from the same raw material (almond shells) and their thermal kinetic behavior is compared with the kinetics of pyrolysis of almond shells. TG–DTG experiments were carried out in order to study the thermal decomposition. Fig. 2 shows the TG–DTG curves of the lignin, almond shells, and holocellulose, and an experiment with the same proportion of lignin and holocellulose in the same sample pan of the TG apparatus, but without contact between the holocellulose and lignin.

The results obtained, and observed in Fig. 2, show that the thermal global decomposition of almond shells cannot be reproduced by adding up the kinetics of decomposi-

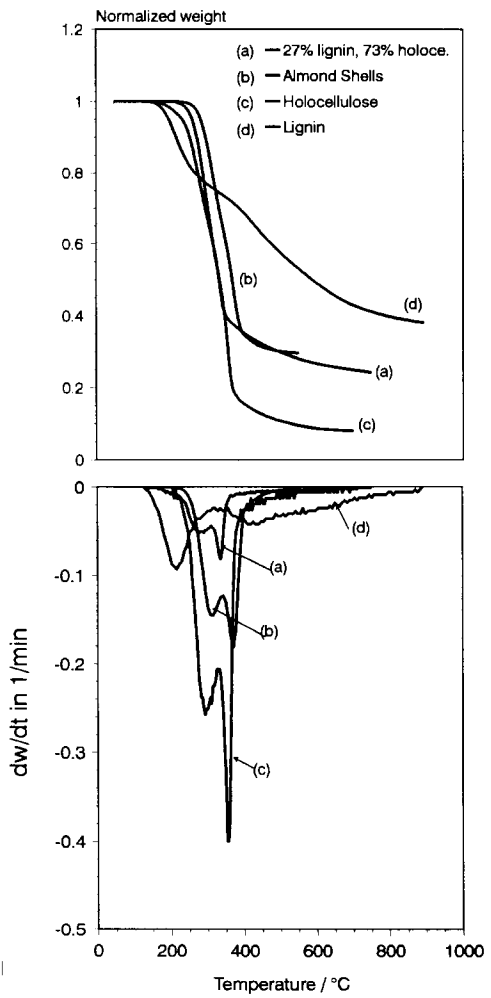

Fig. 2. TG–DTG curves obtained with almond shells, holocellulose, lignin, and lignin (27%) + holocellulose (73%) in the same sample pan, but without contact between them. Heating rate, 10°C min $^{-1}$.

tion of their fractions. As shown in Fig. 2, the simultaneous thermal decomposition of holocellulose and lignin (73 wt% and 27 wt%), in the same sample pan with two independent compartments, does not coincide with the thermal decomposition of almond shells.

In order to explain these results, it is necessary to bear in mind that the structure of the materials can greatly modify the kinetic behavior. For example, Antal [48], in an excellent review of biomass pyrolysis, remarks that there are important differences between amorphous cellulose and crystalline cellulose, both celluloses having the same polymerization degree. In the present work, almond shells were submitted to different chemical treatments in order to separate their fractions. The Kruchner cellulose, which can be considered as a non-degraded or only slightly degraded holocellulose, has a behavior similar to that of almond shells, but decomposes at lower temperatures (shorter times). In almond shells, there is an intact three-dimensional structure with the lignin acting as a cement, and when this cement is eliminated, the thermal decomposition is favored.

The process of lignin isolation requires a severe chemical treatment of almond shells, implying partial depolymerization of the lignin condensations [8] and other chemical transformations. These processes may be the cause of the different pyrolysis behavior observed. At low temperatures, a fast decomposition of volatile groups takes place, probably due to lateral chains in the three-dimensional structure of the lignin [31, 49]. This process seems to be favored in the isolated lignin probably due to the partial polymerization which may take place during the isolation process. However, another process is observed at high temperatures in the case of isolated lignin which seems not to be present in almond shells. This second process might be due to the condensation reactions undergone by the lignin in the isolation process.

However, we believe that if lignin and holocellulose could be isolated without altering their structures, it is probable that the kinetic behavior of that lignin and holocellulose would be different from that when they form part of the almond shells, probably due to strong interactions between holocellulose and lignin in the raw material.

In the holocellulose decomposition, two peaks appear, one due to hemicellulose decomposition and the second due to the cellulose breakdown. The decomposition of holocellulose occurs at lower temperatures than in almond shells (it has a similar qualitative behavior). In the case of lignin, two very well differentiated peaks appear, one at lower temperatures than in cellulose or almond shells, and the other at higher temperatures.

In almond shells, the two peaks in the DTG experiment are probably due to hemicelluloses and cellulose respectively, overlapping with a very wide peak corresponding to the lignin which decomposes throughout the entire process of almond shell pyrolysis.

We suggest that, in the kinetic analysis, the thermal decomposition of almond shells, holocellulose and lignin can be explained by two independent reactions

$$B \rightarrow \nu V + rR$$

$$B \rightarrow \nu' V + r' R \qquad \text{(S1)}$$

where B refers to biomass, V to the volatile matter, R to the solid residue formed, and v, v', r, r' are the yield coefficients, defined as the weight of volatiles (residue) formed divided by the reacted weight of biomass, B.

This scheme of reaction is probably the simplest that includes two processes. In the thermal decomposition of solids, many complex models have been proposed with many kinetic parameters to be optimized. A great number of researchers obtained good results [28, 36, 39, 40, 47, 50], using reaction orders equal to unity or systems of reactions with reaction orders equal to unity. In the present work, the reaction order of each of the two reactions was taken as different from unity, and considered as a parameter to be optimized together with the activation energy and the pre-exponential factor, as will be commented on in the following paragraphs. More complex schemes of reactions have also been tested, including three processes or two processes in which the formation of volatile fraction and char, in each of the individual processes, is produced by two competitive reactions. However the improvement of the adjustment does not justify the increase in the number of adjustable parameters. Under these assumptions, the kinetic equations can be written as

$$\frac{dB}{dt} = -k_{01}\exp\left(-\frac{E_1}{RT}\right)B_1^{n1} - k_{02}\exp\left(-\frac{E_2}{RT}\right)B_2^{n2} \tag{1}$$

$$\frac{dR}{dt} = k_{01}\exp\left(-\frac{E_1}{RT}\right)r_1 B_1^{n1} + k_{02}\exp\left(-\frac{E_2}{RT}\right)r_2 B_2^{n2} \tag{2}$$

where B is the weight fraction of non-reacted biomass (lignin, holocellulose or almond shells) at any moment, B_1 the weight fraction of non-reacted biomass of the first of the reactions considered, B_2 the weight fraction of non-reacted biomass of the second reaction considered; k_{0i} are the pre-exponential factors, E_i the activation energies and n_i are the reaction orders ($i=1, 2$). Note that at time $t=0$, $B_1 + B_2$ equals unity.

The TG experiments cannot differentiate between biomass that has not decomposed at any given moment and the char formed is then usually determined using an equation equivalent to Eqs. (1) and (2) which studies the kinetics of overall decomposition.The weight at any given moment is

$$w = B + R \tag{3}$$

$$\frac{dW}{dt} = -k'_{01}\exp\left(-\frac{E_1}{RT}\right)(w_1 - w_{\infty 1}) - k'_{02}\exp\left(-\frac{E_2}{RT}\right)(w_2 - w_{\infty 2}) \tag{4}$$

where the value w_i is the fraction of biomass that decomposes by the i process and the value of $w_{\infty i}$ is the weight fraction at time infinity, and must coincide with r_i. The equivalence between k' and k (both pre-exponential factors) is

$$k' = \frac{k}{(1-r)^{n-1}} \tag{5}$$

The derivation of Eq. (5) is given in the Appendix.

There are then eight parameters to be optimized, the activation energies, the pre-exponential factors, the orders of reaction; and the other two parameters are the values, $(w_{0i} - w_{\infty i})$ that is the fraction of weight loss due to reaction i.

Flynn [51] showed that in TG experiments, a set of reactions running simultaneously can appear as a single overall process in the TG–DTG curve, and in this case it is possible to describe the behavior of the system using apparent parameters, reaction order, activation energy and pre-exponential factor. Flynn showed that with experiments at different heating rates, it is possible to separate some of these processes, or at least the overall form of the TG–DTG curve is modified. Different researchers [52–55] have shown that an increase in the heating rate causes the TG curves to displace to higher temperatures (when weight loss vs. temperature is plotted). The extent of these displacements depends on the biomass considered.

Therefore, in a possible model that describes the kinetic behavior of biomass decomposition, the kinetic parameters must be constant and not depend on the heating rate. A dependence of the kinetic parameters on the heating rate indicates either bad heat transmission or an incorrect kinetic model. The simultaneous adjusting (the same kinetic constants for all heating rates) of all the TG curves has been proposed as a way to obtain a model which represents the correct kinetic behavior of the sample.

Eq. (4) was integrated using a fourth-order Ruge–Kutta algorithm. The parameters of the model were optimized using a simplex flexible method [56]. The objective function considered was

$$\text{O.F.} = \sum_j \sum_i \left[\frac{\left(\frac{dw}{dt}\right)_{\text{exp}_{ij}} - \left(\frac{dw}{dt}\right)_{\text{cal}_{ij}}}{\left(\frac{dw}{dt}\right)^{\max}_{\text{exp}_j}} \right]^2 \tag{6}$$

where i represents the experimental data at time t in an experiment with a heating rate j (5, 10, 25°C min^{-1}), and $(dw/dt)^{\max}_{\text{exp}\,j}$ represents the maximum experimental rate of decomposition for the experiment with heating rate j. This objective function was chosen in order to correct the effect of the derivatives of w at different heating rates which were different. In this way, the contributions of all the experiments in the objective function are similar. The value of the objective function can be related to the square of a mean relative error of the derivatives. The derivative of the weight fraction with time was chosen because small changes in the weight fraction curve (TG curve) can be better appreciated in the DTG curve, as shown in Figs. 2–8.

A variation coefficient as a statistical parameter was introduced. This parameter analyzes the quality of the adjustment. It is defined as follows

$$\text{V}\cdot\text{C}(\%) = \frac{\sqrt{\frac{\text{O.F.}}{N-P}}}{\left(\frac{dw}{dt}\right)} 100 \tag{7}$$

With holocellulose, the three heating rate runs were correctly adjusted with a model such as that proposed in scheme S1. Table 2 shows the kinetic parameters obtained. Fig. 3 shows the TG–DTG curves and the adjustment obtained. Fig. 4 shows the influence of each of the fractions in the overall decomposition.

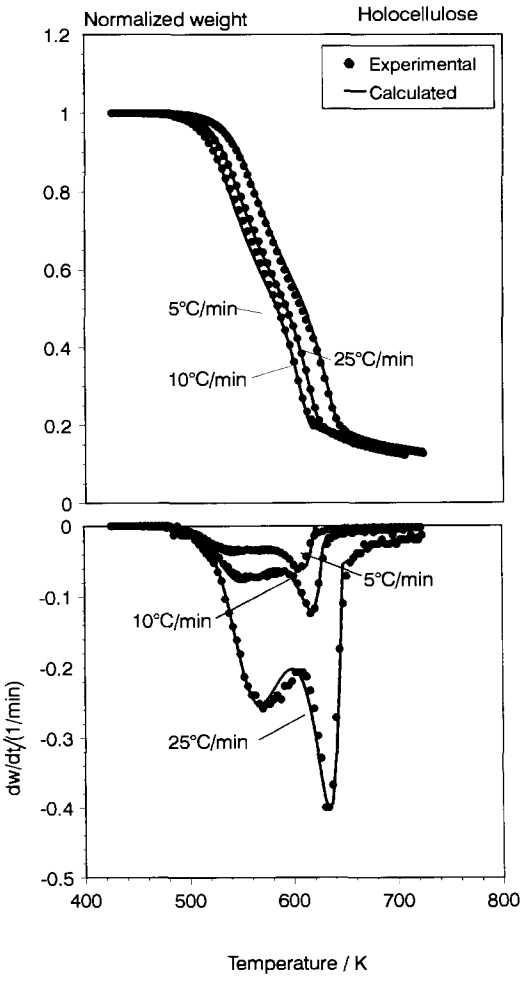

Fig. 3. TG–DTG curves, experimental and calculated, for holocellulose. Points are experimental values and lines are those calculated according to the model.

For almond shells, the adjustment is not as good as in holocellulose. If the TG–DTG curves are analyzed, it is possible to observe that there are two important weight losses (2 peaks in DTG) and a slow weight loss over a wide range of temperatures. This last part of the TG curve is probably due to the lignin fraction which undergoes decomposition over a wide range of temperatures. This weight loss is the same for the three heating rates and is apparently independent of the heating rate. Fig. 5 shows the TG–DTG curves of almond shells and the calculated values. Fig. 6 shows the influence of each of the fractions on the overall decomposition.

Font et al. [47] analyzed the kinetics of the thermal decomposition of almond shells in a TG apparatus. These researchers studied only the two most important weight

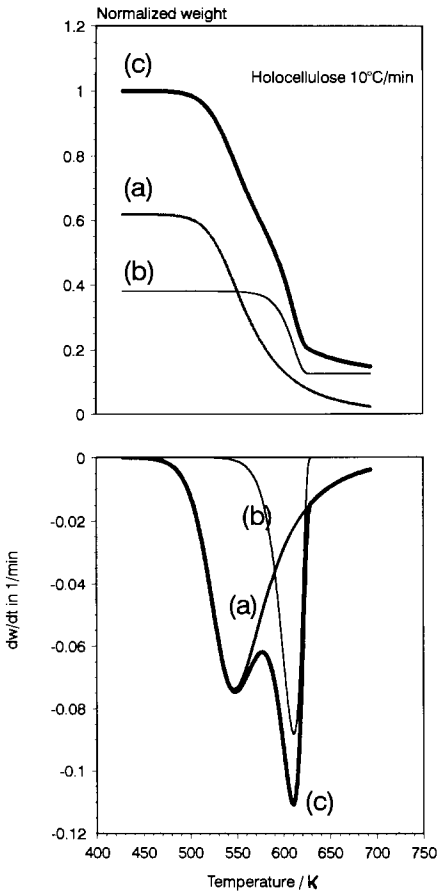

Fig. 4. Influence of each of the two fractions in the thermal decomposition of holocellulose. Values calculated according to the equations of the kinetic model proposed in the text. (a) First fraction. (b) Second fraction. (c) Total decomposition.

losses, but not the final tail of the TG curves. If only these two weight losses are considered, then two first-order independent reactions can describe the process. However, when this tail is considered, it seems that the first weight loss continues until the tail is formed, probably due to reactions that only take place at high temperatures.

With lignin, the model proposed only adjusts one of the TG curves satisfactorily. Fig. 7 shows the experimental and calculated values with the parameters presented in Table 2. It can be observed that the apparent activation energies do not change considerably with heating rate, and that the other parameters are of the same order of magnitude. The difficulty in correlating the experimental data of several runs with different heating rates lies in the fact that lignin decomposes across a very wide range of temperatures. Other models have been proposed in the literature for the thermal decomposition of lignin, admitting variations of the kinetic parameters with conver-

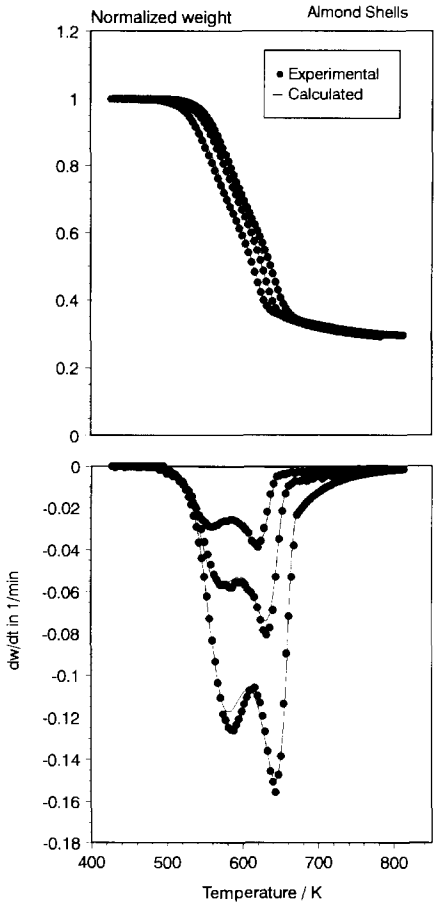

Fig. 5. TG–DTG curves, experimental and calculated, for almond shells. Points are experimental values and lines are those calculated according to the model.

sion [43] or admitting that there is a maximum temperature at which a given fraction of lignin can begin to decompose [57]. Fig. 8 shows the influence of each of the fractions in the global decomposition.

From the kinetic parameters obtained in Table 2 it can be observed that:

(i) The kinetic parameters of almond shells are intermediate between those of holocellulose and lignin, although closer to those of holocellulose, which represents 73% of the almond shells.

(ii) Although there is some similarity between almond shells and the weighed sample of holocellulose and lignin, the entire biomass has a specific behavior due to the interactions of the different fractions.

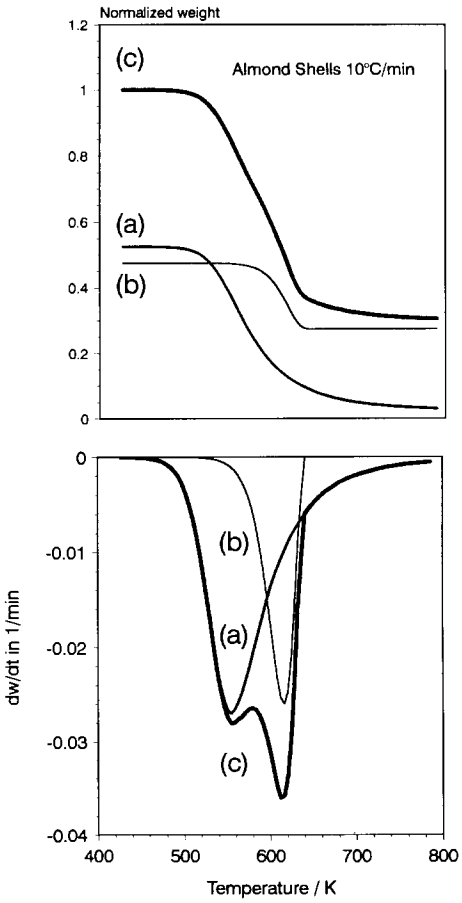

Fig. 6. Influence of each of the fractions in the thermal decomposition of almond shells. (a) First fraction. (b) Second fraction. (c) Total decomposition.

(iii) In general, the kinetic parameters obtained are in accordance with others proposed in the literature for holocellulose, lignin, and different biomasses, see Tables 1 and 2.

4. Conclusions

Taking into account the primary yields obtained with the Pyroprobe (high heating rate) and comparing the results obtained from the weighed sum of holocellulose and lignin, the following can be deduced:

(i) The almond shell yields of propylene, ethane and methanol + formaldehyde are higher than those calculated by adding up the individual yields expected from holocellulose and lignin.

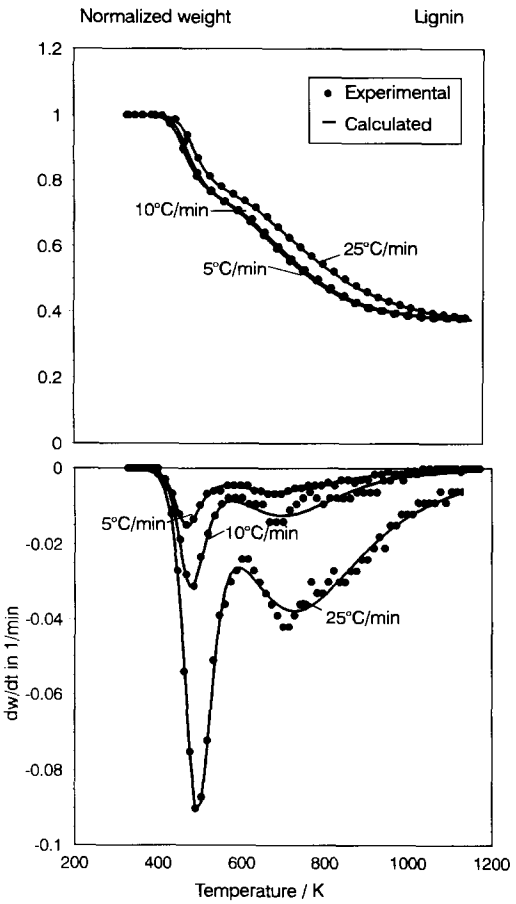

Fig. 7. TG–DTG curves, experimental and calculated, for lignin. Points are experimental values and lines are those calculated according to the model.

(ii) With CO_2, water and CO, a very good correlation is obtained between results from almond shells and from their fractions, indicating that the separation process does not alter the formation of these products.

(iii) Yields of methane in almond shells are an intermediate value between those calculated from their fractions, holocellulose and lignin.

The kinetic behavior in TG runs of the components of biomass (holocellulose and lignin) is different in native conditions than when isolated from the raw material. The separation process modifies the structure of the native compounds of the biomass (in lignin this effect is most important, producing chemically significant changes in its structure) and removes the interactions between fractions.

The kinetic behavior of lignocellulosic biomass and its components, holocellulose and lignin, can be reproduced assuming two independent fractions which decompose simultaneously.

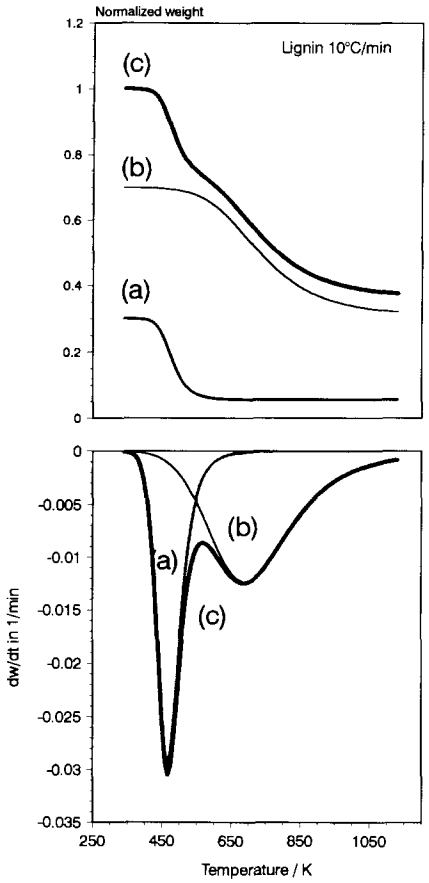

Fig. 8. Influence of each of the fractions in the thermal decomposition of lignin. (a) First fraction. (b) Second fraction. (c) Total decomposition.

Table 2
Parameters obtained in the model

	Holocellulose	Almond shells	Lignin		
			5°C min	10°C min^{-1}	25°C min^{-1}
k_{01}/min^{-1}*	1.44×10^{17}	1.53×10^{11}	7.07×10^{9}	5.05×10^{9}	0.84×10^{9}
E_1/kJ mol^{-1}	177.5	123.6	89.0	87.7	81.7
n_1	3.73	2.58	1.92	1.86	1.44
w_{01}-$w_{\infty 1}$	0.60	0.49	0.20	0.22	0.185
k_{02}/min^{-1}*	6.66×10^{20}	2.03×10^{16}	6.46	24.69	62.2
E_2/kJ mol^{-1}	248.5	199.6	28.1	31.6	30.91
n_2	0.86	1.11	1.42	1.51	1.85
w_{02}-$w_{\infty 2}$	0.27	0.21	0.43	0.41	0.47
O.F.	2.72×10^{-2}	1.57×10^{-2}	8.0×10^{-4}	1.1×10^{-3}	5.6×10^{-4}
V.C. %	2.54	1.33	0.33	0.38	0.33

* Real unit: $min^{-1}(W)^{1-n}$

Appendix

If it is admitted that a solid decomposes according to the follow scheme of reactions

$$B_1 \xrightarrow{k_1} s_1 \text{ Solid} + (1 - s_1) \text{ Volatiles}$$

$$B_2 \xrightarrow{k_2} s_2 \text{ Solid} + (1 - s_2) \text{ Volatiles}$$

where s_i ($i = 1, 2$) is a yield coefficient, defined as kg of solid formed/kg of fraction i decomposed.

With f_{01} the fraction of initial biomass B_{01} with respect to the total initial biomass $B_{01} + B_{02}$ and f_{02} defined similarly, it follows that

$$f_{01} + f_{02} = 1 \tag{A1}$$

With the thermobalance, it is not possible to differentiate the char formed from the non-decomposed biomass, so the kinetics of overall weight loss must be considered. The kinetic equations of each process are

$$\frac{dB_i}{dt} = -k_i B_i^{ni} \tag{A2}$$

$$\frac{dS_i}{dt} = s_i B_i^{ni} \tag{A3}$$

Recalling that the thermobalance weight is the sum of the char formed and the non-decomposed biomass, then

$$w_i = B_i + S_i \tag{A4}$$

Consequently

$$\frac{dw_i}{dt} = \frac{dB_i}{dt} + \frac{dS_i}{dt} = -k_i B_i^{ni}(1 - s_i) \tag{A5}$$

However

$$w_i = B_i + S_i = B_i + (1 - B_i)s_i \tag{A6}$$

From Eq. (A6)

$$B_i = \frac{w_i - s_i}{1 - s_i} \tag{A7}$$

At time infinity, all the biomass has decomposed; therefore the weight then coincides with the weight of char (solid) formed

$$s_i = S_{i\infty} = w_{i\infty} \tag{A8}$$

From Eqs. (A5), (A7) and (A8)

$$\frac{dw_i}{dt} = -k_i\left(\frac{w_i - w_{i\infty}}{1 - w_{i\infty}}\right)^{n_i}(1 - w_{i\infty}) \tag{A9}$$

and calling

$$k_i' = \frac{k_i}{(1 - w_{i\infty})^{n_i - 1}} \tag{A10}$$

then

$$\frac{dw_i}{dt} = -k_i'(w_i - w_{i\infty})^{n_i} \tag{A11}$$

where w_i is the weight of fraction i present at any moment in the sample pan, and $w_{\infty i}$ is the weight of char formed by reaction i at time infinity.

Acknowledgements

Support for this work was provided by CYCIT- Spain, Research project AMB93-1209.

References

[1] A.V. Bridgwater and J.L. Kuester (Eds.), Research in Thermochemical Biomass Conversion, Elsevier Applied Science, London, 1988.
[2] F. Shafizadeh and G.D. McGinnis, Carbohydr. Res., 16 (1971) 273–277.
[3] P. Williams and S. Besler, Thermogravimetric analysis of the components of biomass, in A.V. Bridgwater (Ed.), Advances in Thermochemical Biomass Conversion, Vol. 2, Blakie Academic and Professional, Cambridge University Press, Cambridge, 1992, p. 771–783.
[4] G. Maschio, A. Lucchesi and C. Koufopanos, Study of the kinetic and transfer phenomena in the pyrolysis of biomass particles, in A.V. Bridgwater (Ed.), Advances in Thermochemical Biomass Conversion, Vol. 2, Blakie Academic and Professional, Cambridge University Press, Cambridge, 1992, p. 746–759.
[5] ASTM 1105–56, Standard Method for Preparing Extractive Free Wood, 1972.
[6] B.L. Browning, Methods of Wood Chemistry, Interscience Publishers, John Wiley and Sons, New York, 1965.
[7] TAPPI. Pentosans in Wood and Pulp T223 os 78, 1978.
[8] R.J. Evans, T.A. Milne and M.N. Soltys, J. Anal. Appl. Pyrol., 9 (1986) 1143.
[9] F. García, F. Martín and J.J. Rodríguez, Ing. Quim., (1984) 249.
[10] J.A. Caballero, R. Font, A. Marcilla and A.N. García, J. Anal. Appl. Pyrol., 27 (1993) 221–224.
[11] A.N. García, R. Font and A. Marcilla, J. Anal. Appl. Pyrol., 23 (1992) 99
[12] J. Devesa, Producción de Gases por Pirólisis de Cáscara de Almendra a Elevadas Temperaturas, Ph.D. Thesis, University of Alicante, 1990.
[13] R. Font, A. Marcilla, E. Verdú and J. Devesa, Ind. Eng. Chem. Res, 29 (1990) 1846–1855.
[14] T. Funazukuri, R.R. Hudgins and P.L. Silveston, Symp. Energy from Biomass Waste, III (1984) 589.
[15] Y.L. Stephen and S. Ilona, from Ullmans Encyclopedia of Industrial Chemistry.
[16] S.L. Madorsky, V.E. Hart and S. Strauss, J. Res. Natl. Bur. Stand., 56 (1956) 343.

[17] F.J. Kilzer and A. Broido, Pyrodynamics, 2 (1965) 151.
[18] P.K. Chaterjee and C.M. Conrad, Textile Res. J., 36 (1966) 487.
[19] A.E. Lipska and W.J. Parker, J. Appl. Polym. Sci., (1969) 851.
[20] A.G. W. Bradbury, Y. Sakai and F. Shafizadeh, J. Appl. Polym. Sci., (1979) 3271.
[21] A. Broido, in F. Shafizadeh, K. Sarkanen and D. Tilman (Eds.), Thermal Uses and Properties of Carbohydrates and Lignites, Academic Press, New York, 1984.
[22] R.K. Agrawal, Ph.D. Thesis, Clarkson University, New Kork, 1984.
[23] A. Broido and M.A. Nelson, Comb. Flame, 24 (1975) 263.
[24] P.K. Chaterjee, J. Appl. Polym. Sci., 12 (1968) 487.
[25] R.K. Agrawal, Can. J. Chem. Eng., 66 (1988) 413.
[26] R.K. Agrawal, Can. J. Chem. Eng., 66 (1988) 403.
[27] S.S. Alves and J.L. Figueiredo, J. Anal. Appl. Pyrol., 17 (1989) 37.
[28] D.F. Arsenau, Can. J. Chem. Eng., 49 (1971) 632.
[29] G. Varhegyi and M.J. Antal, Energy and Fuels, 3 (1989) 329.
[30] P.C. Lewellen, W.A. Peters and J.B. Howard, 16th Int. Symp. on Combustion, The Combustion Institute, Pittsburg PA, (1977) 1471.
[31] M.J. Antal, H.L. Fiedman and F.E. Rogers, Combust. Sci. Technol., 21 (1980) 141.
[32] M.T. Klein and P.S. Virk, Energy Lab. Report MIT-EL-81-005, 1981.
[33] E.M. Suuberg, W.A. Peters and J.B. Howard, Ind. Eng. Chem. Process Des. Dev., 17 (1978) 37.
[34] G.E. Domberg and V.N. Seergeva, J. Thermal Anal., 1 (1969) 53.
[35] H.F.J. Wenzl, The Chemical Technology of Wood, Academic Press, New York, 1970.
[36] W.K. Tang, Dept of Agriculture, Forest Serv. Res. Paper, FPL 71, Forest Prods. Lab. Madison, WI, 1967.
[37] M.G. Essig and G.N. Richards, Carbohydr. Res., (1988).
[38] F. Shafizadeh, C.W. Philpot and N. Ostojic, Carbohydr. Res., (1971) 279–287.
[39] M.V. Ramiah, J. Appl. Polym. Sci., 14 (1970) 1323–1337.
[40] A.F. Roberts, Comb. Flame, 14 (1970) 261–272.
[41] J.A. Conesa, J.A. Caballero, A. Marcilla and R. Font, Thermochim. Acta, 254 (1995) 175–192.
[42] M.R. Hajaligol, J.B. Howard, J.P. Longwell and W.A. Peters, Ind. Eng. Chem. Process Des. Dev., 21 (1982) 457–465.
[43] E. Avni and R.W. Coughlin, Thermochim. Acta, 90 (1985) 157–167.
[44] A.J. Stamm, Ind. Eng. Chem., 48 (1956) 413.
[45] B.B. Kreiger and R.W.C. Chen, J. Appl. Polym. Sci., 26 (1981) 153.
[46] T. Hirata and A. Hiroshi, Gov. Forest Exp. Stn. Tokyo, Mokuzai Gakkaishi, 19(9) (1973) 451–459.
[47] R. Font, A. Marcilla, E. Verdú and J. Devesa, J. Anal. Appl. Pyrol., (1991) 249–264.
[48] M.J. Antal, Jr., in Advances in Solar Energy, Vol. 1, Biomass Pyrolysis. A Review of the Literature. Part 1, Carbohydrate Pyrolysis, (1983) 61–111.
[49] M.J. Antal, Jr., in Advances in Solar Energy, Vol. 1, Biomass Pyrolysis. A Review of the Literature. Part 2, Lignocellulose Pyrolysis, (1983) 175–225.
[50] P.T. Williams and B. Serpil, Fuel, 72 (1993) 151–159.
[51] J.H. Flynn, Thermochim. Acta, 37 (1980) 225.
[52] N. Koga, J. Sesták and J. Málek, Thermochim. Acta, 188 (1991) 333.
[53] A.N. García, Estudio termoquímico y cinético de la pirólisis de residuos sólidos urbanos, Ph.D. Thesis, University of Alicante, 1993.
[54] H.E. Kissinger, Anal. Chem., 29 (1957) 1702–1706.
[55] D. Chen, X. Gao and D. Dollimore, Thermochim. Acta, 215 (1993) 109–117.
[56] D.M. Himmelblau, Process Analysis Statistical Methods, J. Wiley & Sons, New York, 1968.
[57] J.A. Caballero, R. Font, A. Marcilla and J.A. Conesa, Ind. Eng. Chem. Res., (1994), accepted.